

Constructing and Modeling a Chaotic Circuit

Samuel Silva
April 15, 2020

Abstract: Nonlinear circuits are a useful tool for studying chaos where the outputs of the circuit match closely with the theoretical expectations. Chaos can be difficult to study in physical systems, but nonlinear circuits offer undergraduates and students a convenient way to learn and study chaos. We used a circuit design from J.C. Sprott to explore fundamental principals of chaos such as attractors and fractals to observe that sensitive dependence of initial conditions can produce unpredictability in the future.

1. INTRODUCTION

With the growing study of nonlinear analysis in fields of weather, general relativity in astronomy, dynamics of matter waves, and applications in programming such as machine learning, it becomes apparent that many nonlinear systems are ubiquitous [9]. Due to the wide range of these systems, it is important to teach students the principals of nonlinear systems. Many nonlinear systems display chaotic behavior, such sensitive dependence on initial conditions that similar initial states evolve into vastly-different behavior [5]. Due to the underlying principals of chaos and how precise and unique a system must be, it can be a challenging and expensive undertaking to study chaos in physical systems. Experiments have used such mechanical systems as double pendula, flowing fluids, and even bouncing balls to demonstrate valuable techniques to analyze chaos. However, there are difficulties with these experiments since they are subject to outside factors such as friction, unevenness of surfaces, and even variation of gravity, which can make data difficult to reproduce.

Better systems to study chaos are nonlinear electronic circuits which offer increased reproducibility and results that closely match the theoretical expectations. Individual circuit components, such as resistors, are accurately modeled mathematically and that leads to our ability to accurately model whole circuits with differential equations. Circuits become an ideal system to study chaos since the experimental data corresponds closely to the theoretical results, and the experiments can easily be set up and completed in any lab.

In 1983, Leon Chua used a simple design to construct one of the first chaotic circuits. Unfortunately, it was difficult to model since the circuit used an inductor which provides both an impedance and a resistance, therefore it became challenging to scale the circuit to different frequencies. The circuit created by J.C. Sprott [6], is a more user-friendly chaotic circuit and still displays the fundamental behavior of chaos. In addition, the data taken from Sprott's design can precisely demonstrate the chaotic and periodic behavior of the circuit, where a control parameter can be incorporated into the circuit, allowing for the circuit to go in and out of chaos.

2. CHAOS THEORY

2.1. History of Chaos

Starting in the 19th century and gaining traction after Edward Lorenz's paper in 1963, researchers noticed that small uncertainties in an initial state can lead to large uncertainties in a final one. Lorenz is best known for being a pioneer in chaos theory, but there were people like Henri Poincare in the 1880s who noticed similar behavior [2]. Poincare studied the three-body problem in classical mechanics and reported that small differences in the initial conditions produced very great ones in the final phenomena and being able to predict the final outcomes seemed impossible. Dynamical systems like the three-body system that involve taking the initial positions and velocities of three point masses and solving for their subsequent motion, are best described in phase space, where dimensions correspond to the dynamical variables such as positions and velocities. This allows the system to be described by a set of first-order ordinary differential equations. Poincare would fail to mathematically describe his results from the three-body trajectories and the reasoning why it was difficult to model the trajectories, but his findings would hint at chaos.

Edward Lorenz was a meteorologist and joined MIT faculty in 1955. At this time meteorologists used linear models to predict the weather, believing tomorrow's weather should be a well-defined linear combination of features of today's weather [2]. However, Lorenz would also work on creating nonlinear models. He searched for

nonperiodic solutions to his linear model and found that by adding an external heating that varied with latitude and longitude, he received a significantly different result than the original linear model [3]. Continuing his study of his nonperiodic model, Lorenz would reproduce data from the simulated weather and would round off each day's results to the third decimal place. He was surprised that when he repeated the processes, but retained more decimals, he received drastically different results [2]. This phenomena would be the foundation for his landmark paper in 1963 [3]. Lorenz nicknamed this behavior the “butterfly effect” suggesting sensitive dependence on initial conditions.

Many areas of physics deal with nonlinear problems, but it is important to make the distinction between chaos and non-linearity. For example, a chaotic system is also a nonlinear system, but not every nonlinear system is a chaotic system because it lacks the predefined characteristics. Section 2.2 provides information on what characteristics researchers look at to gauge if a system is chaotic.

2.2. Characteristics of Chaos

Defining characteristics of a chaotic system include the system's being extremely sensitive to initially conditions which makes it nearly impossible to predict the long term behavior of the system. One of the difficulties when modeling chaos arises from this trait, where the smallest of mistakes will be amplified when computing the system's results. Other characteristics include [9]:

1. never repeating
2. allowing for short term prediction but long term unpredictability
3. the system moves in and out of chaotic states caused by the changing of the control parameter
4. can produce a fractal pattern

Fractals are complex geometric shapes with a fine structure and no characteristic scale length. A popular example illustrating the lack of scale length is the coastline paradox, where the ruggedness of boulders and sand on small and large scales look the same. Fractal structures can be used to find a strange attractor in experimental data [7], where an attractor is a set of values which a system tends to evolve towards. Attractors and other methods of visualizing and studying chaos are described in sections 2.3, 2.4, and 2.5, but it is important to understand what fractals are and when they appear, since they show up in many areas of chaos theory. Fractals are of great interest to mathematicians because of their unique complexity and endless structure, but also to geophysicists and other physicists Figure 1. Objects in nature ranging from trees, coastlines, rivers, and clouds, exhibit self-similar features [1], supporting the need to be able to study chaos on a smaller scale in a laboratory setting before applying it large scale research.

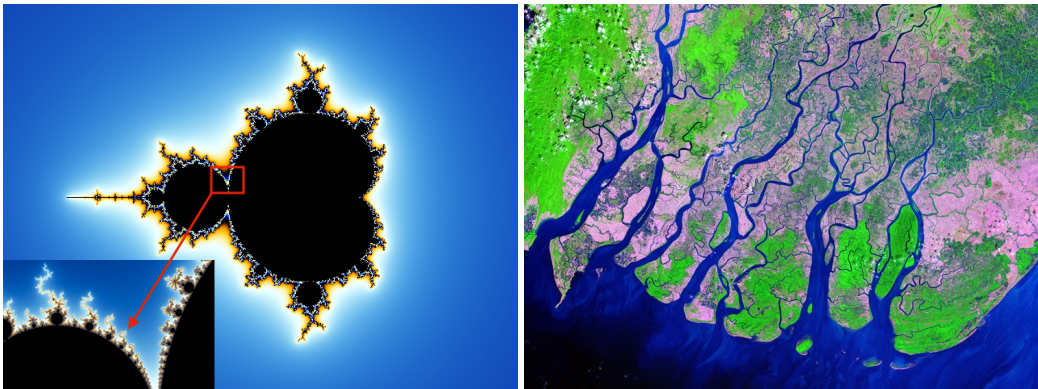


Figure 1: Fractals from the Mandelbrot set: exhibit an elaborate and infinitely complicated boundary that reveals progressively ever-finer recursive detail at increasing magnification (left). NASA image of the Ayeyarwady River Delta displays the fractal branching patterns of river delta ecosystems (right).

A general property that most fractals possess is a degree of self-similarity, suggesting that small sections of an object resemble the whole object [9]. The study of fractals is vast and goes beyond the scope of this section, the take away should be that fractals have a fine shape upon magnification and appear in many areas of chaos and even nature.

2.3. Attractors

One of the most popular images in chaos is the Lorenz Attractor, which demonstrates the behavior of his equations.

Lorenz Equations:

$$\begin{aligned}\frac{dx}{dt} &= \sigma(y - x) \\ \frac{dy}{dt} &= rx - y - xz \\ \frac{dz}{dt} &= xy - bz\end{aligned}$$

Attractors can be a helpful tool to visualize the directional behavior of a system. For example, using the Lorenz equations, points of x, y, z can be plotted in phase space. The visual resulting from Lorenz Equations can be seen in Figure 2. In general, attractors are a set of numerical values where all neighboring trajectories converge [9]. More specific descriptions of attractors include:

1. A is an invariant set where any trajectory $\mathbf{x}(t)$ starts and remains in A .
2. A attracts an open set of initial conditions. Essentially, A will attract all trajectories that start relatively close to it.
3. A is minimal, therefore, no proper subset of A will satisfy conditions 1 and 2.

To be an attractor, the set must meet all three characteristics. A specific case of attractors are called strange attractors which can contain a fractal structure. An attractor can also be a point, a finite set of points, a curve, or even a manifold residing in topological space. Strange attractors demonstrate sensitive dependence to initial conditions, one of the fundamental characteristics of a chaotic system. Chaotic attractors are embedded with an infinite number of unstable periodic orbits. The Lorenz System is considered to be a strange attractor, Figure 2, where Lorenz believed that a single feature of a given "loop" would predict the feature of the following circuit [9]. The idea of predicting features will be explained in greater detail in the Return Maps section.

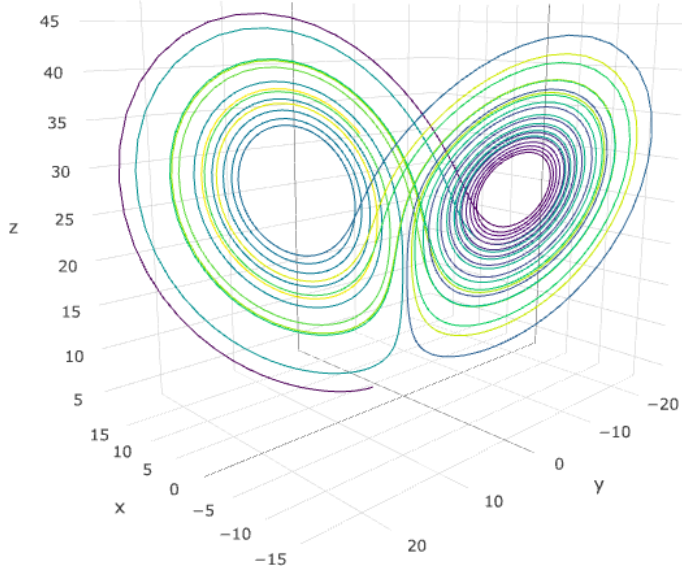


Figure 2: Lorenz's attractor, nicknamed "The Butterfly Curve" for its shape.

Other general uses of attractors include being able to distinguish between stable and chaotic states. A stable state would result in a plot of a closed loop while a chaotic state in a non-closed loop. In addition, attractors can demonstrate period-doubling, occurring by changing the initial parameter which causes new behavior with twice the period of the original state. Period-doubling can also be seen in other chaotic system analyses such as in power spectra analysis and bifurcation diagrams.

2.4. Nonlinear Time Series

Time series analysis allows for the creating of return maps Figure 3, and power spectra analysis seen in Figure 4. If one imagines the looping trajectory of Figure 2 being drawn in real time, then Figure 3a would be produced by just recording how the z component evolves over time. A raw time series such as this may seem too complex to reflect simple, underlying principals, but the corresponding return map (Figure 3b) and power spectra yield insights. One of Lorenz's historical contributions to chaos theory was that he was able to find order from chaos. He presumed the peak z_n (Figure 3a) in the time series would predict z_{n+1} , and ultimately used this to map chaos by plotting the peak versus the previous peak of the time series. Mapping his equations yielded a function [9] $z_{n+1} = f(z_n)$ shown in Figure 3.

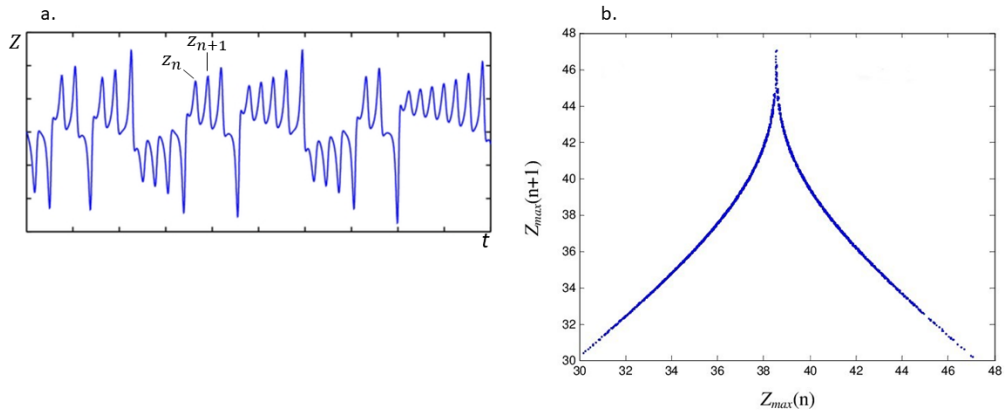


Figure 3: Lorenz time series (a) and the resulting *Lorenz Map* (b)

It is apparent that the curve in the Lorenz map has some 'thickness' to it so $f(z)$ is not a well-defined function [9]. The thickness occurs since there are multiple outputs z_{n+1} for any given input z_n . The general name for the plot of peaks versus the previous peaks of the time series is called a return map. A return map offers a unique way to visualize chaos and has the benefit a discrete, one-dimensional map of chaos, and can often display a fractal structure. Return maps are interesting to use for chaotic states because if a map was made from a stable state, one would see only a few distinct points for however many peaks the time series has.

Another use a of time series is the creating of a power spectrum that takes the Fourier transform to describe the distribution of power into frequency components composing that signal [4]. The higher the peak, the more energy there is at that frequency. It is expected for stable states that the power spectra has a few distinct peaks, while for a chaotic state the spectra lacks defined peaks because the energy is unevenly distributed across the system. Power spectra also reveals period doubling where the number of peaks will double between as the control parameter is varied.

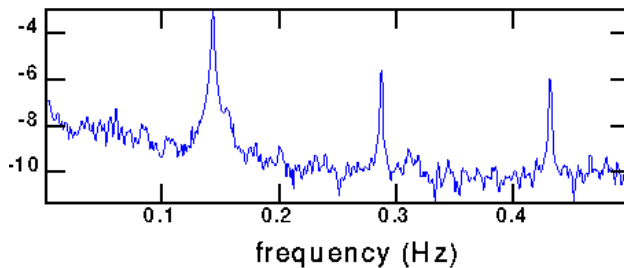


Figure 4: Time series where the higher the peak, the higher the energy.

Bifurcation diagrams will also show period doubling. This type of plot is used to visualize the behavior for various values of the control parameter. Since chaotic systems are nearly impossible to predict, there is some value to have a plot that displays the entire behavior of a system. Similar to the return maps, bifurcation diagrams are constructed from the peaks of a time series at a specific value of the initial condition. For the same reason

why the return maps appear dense, there are multiple outputs for a particular output, however, the bifurcation diagram plots the outputs at its natural location. For example, if we look at the bifurcation diagram for the Lorenz equations, we see that at $r = 165$ there are four distinct points which will correspond to four repeated peaks of the time series when $r = 165$. At point $r = 175$ we see countless points suggesting the system is in a chaotic state and that the time series would display an extreme variety of peaks where almost none are repeating.

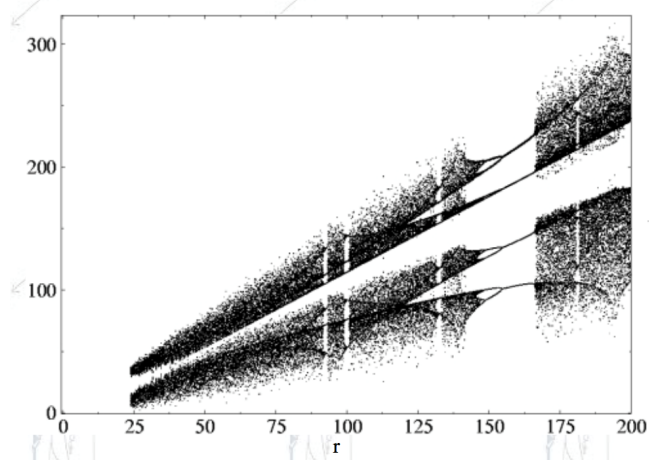


Figure 5: Bifurcation diagram for the Lorenz system. Dense vertical bands are chaotic states for the varying parameter r , and bands of white with distinctive lines are stable regions [5].

2.5. Lyapunov Exponent

Another way to examine chaos is to see if the motion of the attractor exhibits sensitive dependence on initial conditions. This is achieved by calculating the exponential divergence of nearby trajectories, dubbed the Lyapunov exponent. In other words, as two trajectories start extremely close together on the attractor, they will rapidly diverge from one another and have very different results [9]. Lyapunov exponents will always be real numbers and their directions would change as a result of the trajectory moving through space, where their directions are perpendicular to the orbits of the attractor. Furthermore, a system with n dimensions will have n Lyapunov exponents, similar to how it would have n eigenvalues at each point [7].

Table 1: δ Comparison of eigenvalues and Lyapunov exponents [6]

EigenValue	Lyapunov exponent
<i>Local</i> quantity	<i>Global</i> quantity
<i>Constant</i> value	<i>Average</i> value
<i>Complex</i> number	<i>Real</i> number
<i>Not</i> usually orthogonal	Mutually <i>orthogonal</i>

To mathematically understand how to calculate the Lyapunov exponent, suppose $\mathbf{x}(t)$ is a point on an attractor at time t , where there is a neighboring point is $\mathbf{x}(t) + \delta(t)$. There is a small separation between the points, δ , which is visualized in Figure 5.

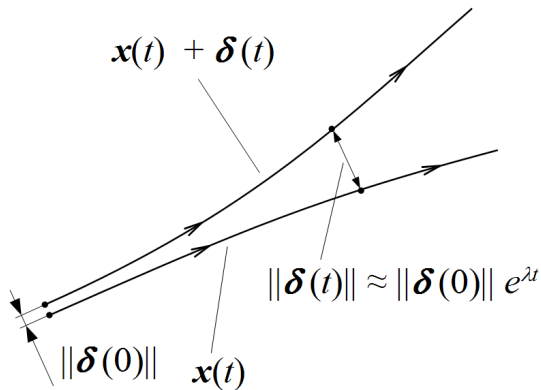


Figure 6: Diagram of the trajectories used in the calculation of the Layapunov exponent.

As $\delta(t)$ grows, numerical studies have shown

$$\|\delta(t)\| \approx \|\delta(0)\| e^{\lambda t}. \quad (1)$$

It is important to note that λ commonly represents the Lyapunov exponent, however, λ is typically used to represent the largest measured Lyapunov exponent. We already know that there are actually n different Lyapunov exponents for an n -dimensional system, where all Lyapunov exponents will measure the separation trajectories in their relative dimension. In most cases, the largest λ is a sufficient measurement, but mathematicians and researchers have also averaged over multiple points to get a more accurate measure of λ . Looking back at equation 1, a positive exponent would yield exponential growth in the separation, thus two trajectories would continue to separate, as in chaos, and a negative exponent would yield exponential decay, bringing two trajectories to each other in a stable orbit. This can be applied to the Lorenz attractor with an initial separation length of $\|\delta(0)\| = 10^{-15}$, resulting in a Lyapunov exponent of $\lambda = 0.9$.

3. THE NONLINEAR CIRCUIT

3.1. Circuit Design

Now that chaos has been briefly described along with various analyses and calculations that can be done, we can start to look at Sprott's circuit [6]. A third order differential equation can be used to describe a class of circuits that can display chaotic behavior. The equation is one of these differential equations where x is the voltage at a specific node that corresponds to the circuit. In Equation 1, both A and α are constants and $D(x)$ is a nonlinear function in the differential equation. Furthermore, the derivatives of x are taken with respect to dimensionless time.

The proposed circuit from J.C. Sprott models the class of circuits using Equation 1 [6]. The schematic of the circuit can be found in Figure 7.

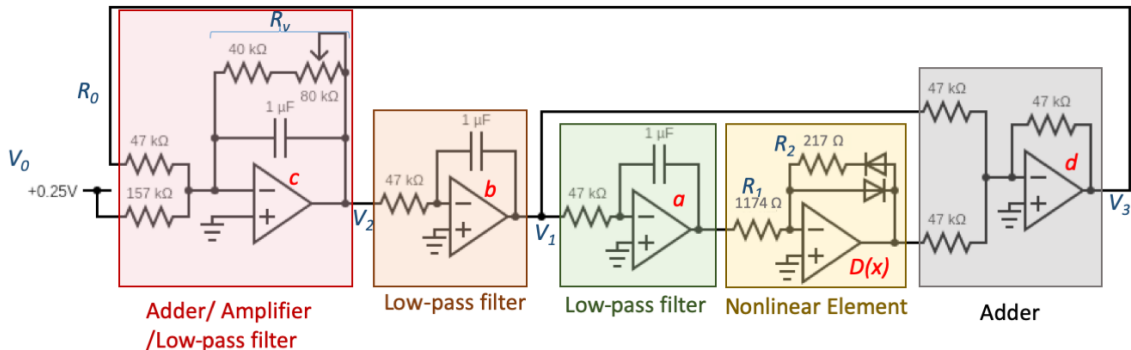


Figure 7: General schematic of the chaotic circuit proposed by J.C. Sprott.

The actual details of the circuit are described later on in the Procedure section, but V_0 is the input voltage and R_v is the variable resistance and control parameter. Any unlabeled resistor R or capacitor C have the same resistance or capacitance, respectively. From Equation 2, $D(x)$ is a nonlinear function which can be modeled with its own subcircuit in Figure 8. The placement of $D(x)$ in the larger circuit can be found in Figure 7.

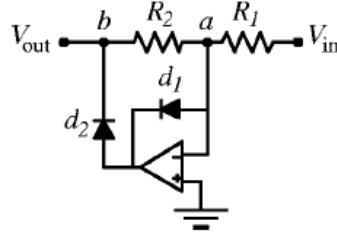


Figure 8: Schematic for the nonlinear element. Is made up of an op-amp, two diodes, and two resistors.

The subcircuit $D(x)$ is fundamental for the circuit to display chaotic behavior where the voltage at the output of $D(x)$ is related to its input by,

$$V_{out} = D(V_{in}) \quad (2)$$

The general circuit can be written using the "golden rules" of op-amps consisting of:

1. The op-amp has infinite open-loop gain.
2. The input impedance of the +/- inputs is infinite. The output impedance is zero.
3. No current flows into the +/- inputs of the op amp.
4. In a circuit with negative feedback, the output of the op amp will try to adjust its output so that the voltage difference between the + and - inputs is zero ($V_+ = V_-$).

Using these rules, the relation to op-amp "a" is

$$V_1 = -R_a C_a \frac{dx}{dt}, \quad (3)$$

for op-amp "b" is

$$V_2 = -R_b C_b \frac{dV_1}{dt}, \quad (4)$$

for op-amp "c" is

$$C_c \frac{dV_2}{dt} = -\frac{V_2}{R_v} - \frac{V_0}{R_0} - \frac{V_3}{R_c}, \quad (5)$$

and for op-amp "d" is

$$V_3 = \left[\left(\frac{R_d}{R_e} \right) V_1 + \left(\frac{R_d}{R_f} \right) D(x) \right]. \quad (6)$$

We can define the dimensionless variable related to time by

$$\tilde{t} = \frac{t}{R_a C_a}. \quad (7)$$

This is defined to make \dot{x} simple. From Equations 3 and 7, we get

$$V_1 = -\frac{dx}{d\tilde{t}} = -\dot{x}. \quad (8)$$

Using Equations 4, 7, and 3, we get

$$V_2 = -\frac{R_b C_b V_1}{R_a C_a d\tilde{t}} = \frac{R_b C_b}{R_a C_a} \ddot{x}. \quad (9)$$

From equations 5 and 7, we get

$$\frac{dV_2}{dt} = R_a C_a \frac{dV_2}{dt} = \frac{R_b C_b}{R_a C_b} \ddot{x} = \left(\frac{V_2}{R_v} + \frac{V_0}{R_0} + \frac{V_3}{R_c} \right) \frac{R_a C_a}{C_c}, \quad (10)$$

or

$$\ddot{x} = - \left(\frac{R_c}{R_v} V_2 + \frac{R_c}{R_0} V_0 + V_3 \right) \frac{R_a^2 C_a^2}{R_b R_c C_c}. \quad (11)$$

Substituting Equations 6, 8, and 9 into Equation 11 gives

$$\ddot{x} = \left[- \left(\frac{R_c}{R_v} \frac{R_b C_b}{R_a C_a} \right) \ddot{x} - \left(\frac{R_d}{R_c} \right) \dot{x} + \left(\frac{R_d}{R_f} \right) D(x) - \left(\frac{R_c}{R_0} \right) V_0 \right] \frac{R_a^2 C_a^2}{R_b C_b R_c C_c}. \quad (12)$$

Equation 12 is used when wanting to model the circuit as accurately as possible, because there are minor variations in the unlabeled resistors and capacitors. The nonlinearity of the circuit, $D(x)$, takes the value of an absolute value, thus $D(x) = |x|$. However, this form would cause the solutions of the the differential equation to become unbounded when R_v exceeded a certain threshold [6]. More specifically in the proposed model, the function takes the form $D(x) = -6\min(x, 0)$ and leads to no unbounded solutions. The -6 is a ratio of R_2 and R_1 .

Variations of $D(x)$ exist and can be applied as AC voltmeters [8]. To demonstrate that the circuit matches the functional form, the Shockley equation can be employed to model the $I - V$ curves for the diodes in the subcircuit.

Figure 8 (subcircuit) can be modeled with

$$D(V_{in}) = \begin{cases} 0 & \text{if } V_{in} > 0 \\ \frac{R_2}{R_1} |V_{in}| & \text{if } V_{in} < 0 \end{cases}$$

where the input x and output $D(x)$ produces the plot in Figure 9. We see that there is discontinuity at $x = 0$, thus confirming its nonlinearity.

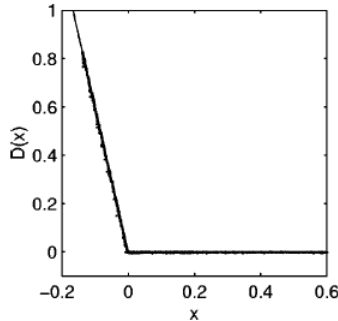


Figure 9

Sprott emphasizes that the point of expression $D(V_{in})$ is that the op-amps in the subcircuit influence the diodes to cause the circuit to become extremely sensitive to the diodes themselves [6].

3.2. Set Up/Procedure

The circuit used in this experiment has a modular and friendly design. Two important components of the circuit are the control parameter, R_v , and the component $D(X)$, which can been seen in Figure 8. The variable resistor is a digital potentiometer that allows for the accurate setting of its resistance.

By changing the resistance of R_v , one can move the system between stable and chaotic states. The component $D(x)$ is a subcircuit that acts as the circuit's nonlinear element. The idea of having a nonlinear component in the the general circuit corresponds to Chua's circuit which also had its own version of a chaotic subcircuit named Chua's Diode. Coincidentally, Sprott's subcircuit is built using nonlinear components such as diodes. The schematic of the general circuit is seen in Figure 8 where the $D(x)$ subcircuit schematic is present in Figure 9.

The general circuit is made of two operational amplifier integrators, an operational amplifier follower, and another version of an integrator that has the variable resistance in parallel. The integrator with R_v can be considered as a normal integrator when the variable resistance is set to 0Ω . Integrators have an important role

in the circuit since op-amps can be used in positive or negative feedback amplifier type circuits, when they just use pure resistances in both the input and the feedback loops [8]. This relates back to the characteristics of chaos where feedback is one of the fundamental characteristics that lead to fractal structures and amplification of small variations in data. Voltage followers are also useful components where the op-amp does not provide any amplification to the signal. The follower also allows the output voltage to directly follow the input voltage, meaning the output voltage is the same as the input voltage. [8]. The nonlinear element of the circuit, $D(x)$ is made up of another op-amp, two diodes, and two more resistors. Diodes allow current to flow in only one direction and since a diode has a variable resistance, it is a nonlinear device. With all these pieces of the circuit together, the goal is to be able to read the voltage signals at points V_1 , V_2 , and V_3 and perform various analyses to study chaos.

3.3. Equipment and Software

The circuit is made up of a collection of resistors, capacitors, operational amplifiers, and diodes. Based on the design by Sprott, the unlabeled resistors were $47\text{k}\Omega$, $R_0 = 157\text{k}\Omega$, and the ratio of $R_2/R_1 \approx 6$. The resistances of R_2 and R_1 can be any value as long as its ratio remained close to 6. Our circuit used $R_1 = 1174\text{\Omega}$ and $R_2 = 217\text{\Omega}$. The capacitors, C , were $1\mu\text{F}$, and R_0 was $157\text{k}\Omega$. The chosen operational amplifiers were the LMC6062 model which have a high input impedance. Other models of op-amps were used such as low noise ones, but LMC6062 produced the most accurate results. Additionally, other capacitors were used ranging from ceramic to paper models, but the ceramic model was the best for the same reason as the op-amps; they produced the most accurate output. Each op-amp had a power supply of $\pm 5\text{V}$. Sprott recommended that the input voltage was $V_0 = 0.250\text{V}$. The variable resistance, R_v , consisted of eight 256-step DS1803 digital potentiometers where each had an approximate resistance of $10\text{k}\Omega$. A Teensy Microcontroller (Figure 11) controlled the potentiometers and recorded the voltages at specific points in the circuit. A $40\text{k}\Omega$ resistor was placed in series at the end of the potentiometers so the resistance ranged from $40\text{k}\Omega$ to $120\text{k}\Omega$, which was important when trying to map all outputs for a wide range of resistances.

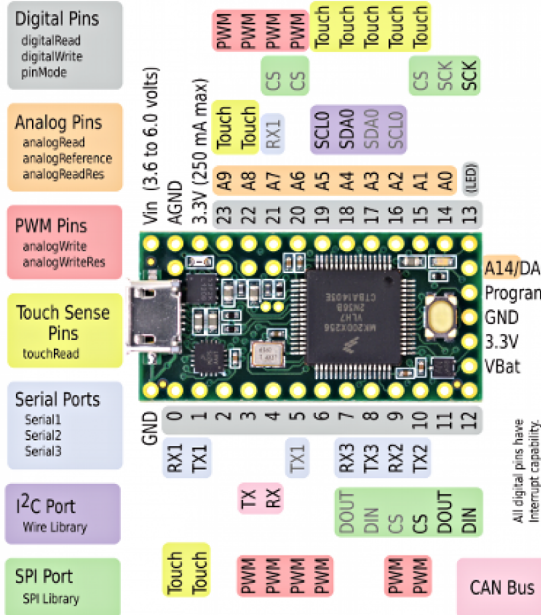


Figure 10: Pin placement of the Teensy 3.2 Microcontroller.

For both controlling the digital potentiometers and recording measurements at V_1 , V_2 , and V_3 , we used a Teensy Microcontroller. We chose the Teensy because of its compact size and its increased resolution compared to microcontroller alternatives. For simplicity and friendliness, it was desired to find a method where one device could do both processes of setting the digital potentiometers and recording measurements, rather than have multiple devices that require their own programming and setting up. Allowing LabVIEW software to control the Teensy, made it possible to accurately set the resistance of R_v and then record the data from all three points in the

circuit. LabVIEW is a system-design platform and development environment for a visual programming language from National Instruments. The Teensy became compatible with LabVIEW by uploading Teensy support code through the Arduino IDE on to the Teensy, where a LabVIEW VI can have control over the microcontroller. This is also where the resolution can be set; the Teensy had a resolution of 12 bits. The resolution refers to how small of values the controller is able to distinguish between, therefore, the higher the resolution then the smaller of a change that can be theoretically detected. To incorporate the Teeny microcontroller into the physical circuit, the analog pins in Figure 11 are connected to connected to V_1 , V_2 , and V_3 , while the digital read and write are connected to the digital potentiometers.

3.4. Incorporating Circuit and Code

Once LabVIEW recognized the Teensy microcontroller, code needed to be written so a signal could be sent to the controller and accurately adjust the resistance of the digital potentiometers. Simultaneously, the controller needs to be able to read the voltage at the desired points in the circuit. The data would be read at a frequency of 180 Hz which was close to the 167Hz used by Sprott. With a multitude of analyses planned, it was necessary to record data efficiently and quickly. By using a LabView, it allowed for the digital potentiometers to be set and for the measurements to be recorded all through the same interface. Along with using the Teensy microcontroller, it was convenient to have one device and one program to do all the tasks. The program allowed for the control over the number of iterations, delay between measurements and setting the resistance, how many resistances to take data from, and the recording of time series data.

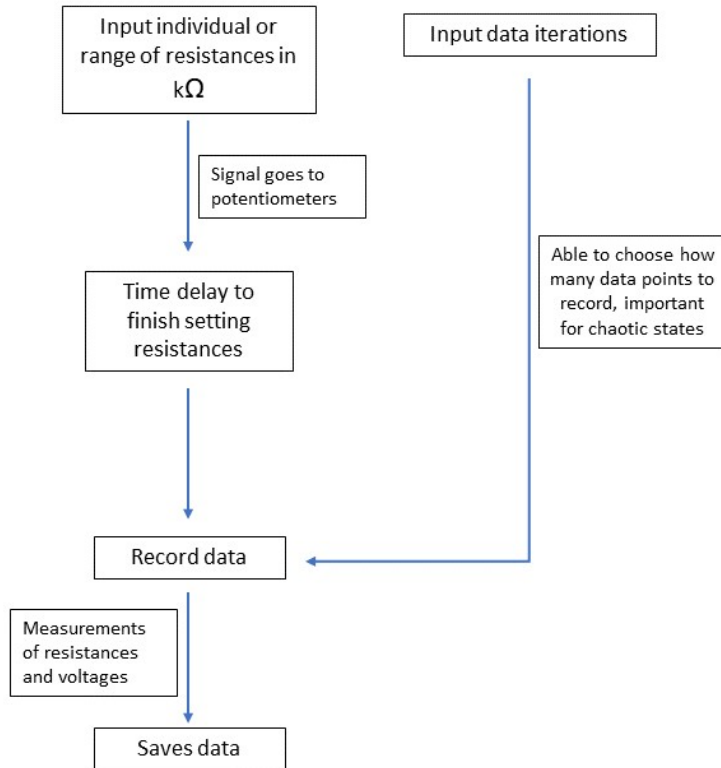


Figure 11: Flowchart of the processes done by LabVIEW. It is important to choose the amount of iterations because chaotic states require more data points to see the whole attractor, while stable states need less points for attractor to take shape.

In the interest of accurately modeling the circuit's behavior, it is necessary to carefully measure each resistor's resistance and capacitor's capacitance before constructing the circuit. When building the circuit it is vital to note that each resistor or capacitor does not have the same exact value, therefore, it is necessary to measure each component separately. An issue that was prevalent in the first few versions of the circuit included a drifting voltage which caused issues when modeling the data. Originally, there was a voltage source for the op-amp power,

and then another power supply used for V_0 and a floating ground. To combat the drifting voltage, only one power source was used where a voltage divider output a 0.250V and a 0.725. The 0.250V was used as V_0 and 0.725 was used as the floating ground. A floating ground was necessary to keep all the measurements positive since the Teensy is only able to read positive signals. Evidently, having only one power source also reduced noise in the circuit.

4. ANALYSIS

Using the measurements from V_1, V_2 , and V_3 , we can compare the experimental data to the computations using taken from equation 13, by using the techniques described throughout Section 2. The analyses include looking at the attractor through phase portraits, power spectra, return maps, bifurcation diagrams, and Lyapunov exponents. We chose to look at each analysis with the control parameter being set to $50\text{ k}\Omega$, $60\text{ k}\Omega$, $72\text{ k}\Omega$, and $80\text{k}\Omega$. To obtain spectral data we used a Stand-ford Research SR770 FFT Spectrum Analyzer, and the remaining analyses were done by running our data through programs in Python.

4.1. Phase Portraits

We made a phase portrait by plotting \dot{x} versus x to visualize the attractor and to view the directional behavior of our system. They are a useful tool for comparing experimental data and the theoretical values determined by the ODE's. Phase portraits are also a method to visualize chaos. Figure 13 shows four phase portraits for four different values of R_v , where $50\text{ k}\Omega$, $60\text{ k}\Omega$, $72\text{ k}\Omega$ are stable states, and $80\text{k}\Omega$ is a chaotic attractor.

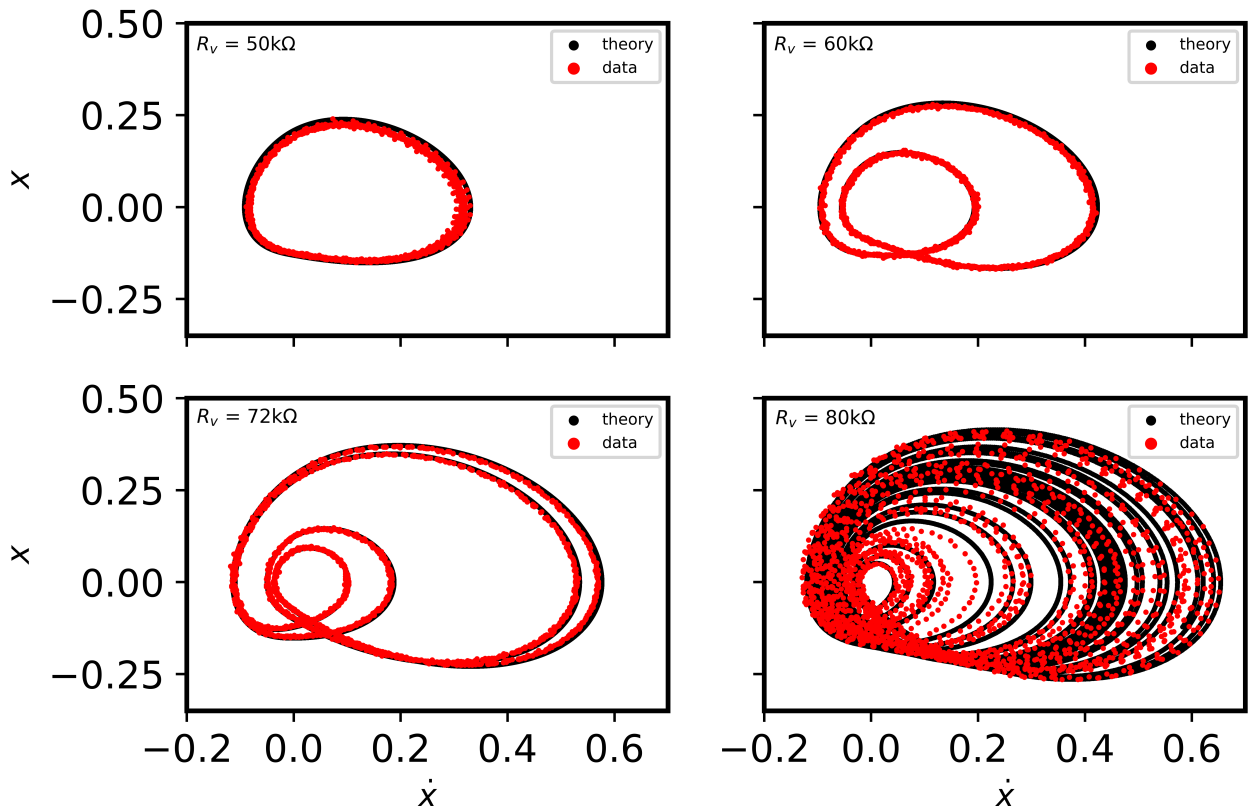


Figure 12: Phase portraits for $50\text{ k}\Omega$, $60\text{ k}\Omega$, $72\text{ k}\Omega$, and $80\text{ k}\Omega$. The experimental data matches closely to the theoretical expectations.

The comparison of the experimental and theoretical attractors are nearly identical for lower values of R_v while there is some discrepancies at higher values. In our phase portraits we see "period doubling." At $50\text{ k}\Omega$ there is a single closed loop suggesting a stable state, and the amount of loops doubles. This occurs by changing the initial parameter which causes new behavior, with twice the period of the original state. We saw that the number of loops doubled as R_v increased to $60\text{ k}\Omega$ and to $72\text{ k}\Omega$, both with a closed loop suggesting stable orbits. However, at $80\text{k}\Omega$

$k\Omega$ we see a chaotic attractor with a non-closed and countless loops. This is also where we see minor imperfections between the experimental and theoretical attractors proving how difficult it is to accurately model any chaotic system. Reasons for slight variation between experimental and theoretical results include noise within the circuit and saturation.

4.2. Power Spectral Density

The power spectra density (PSD) is an analysis where we take the Fourier Transform of our x signal showing the frequencies make up the signal. The higher the peak, the more energy there is at that frequency. We saw "period doubling" again in the PSD analysis, where the number of peaks double from the previous state. For the chaotic state we saw that the signal lacks defined peaks because the energy is unevenly distributed across the circuit. The experimental results can be found in Figure 14.

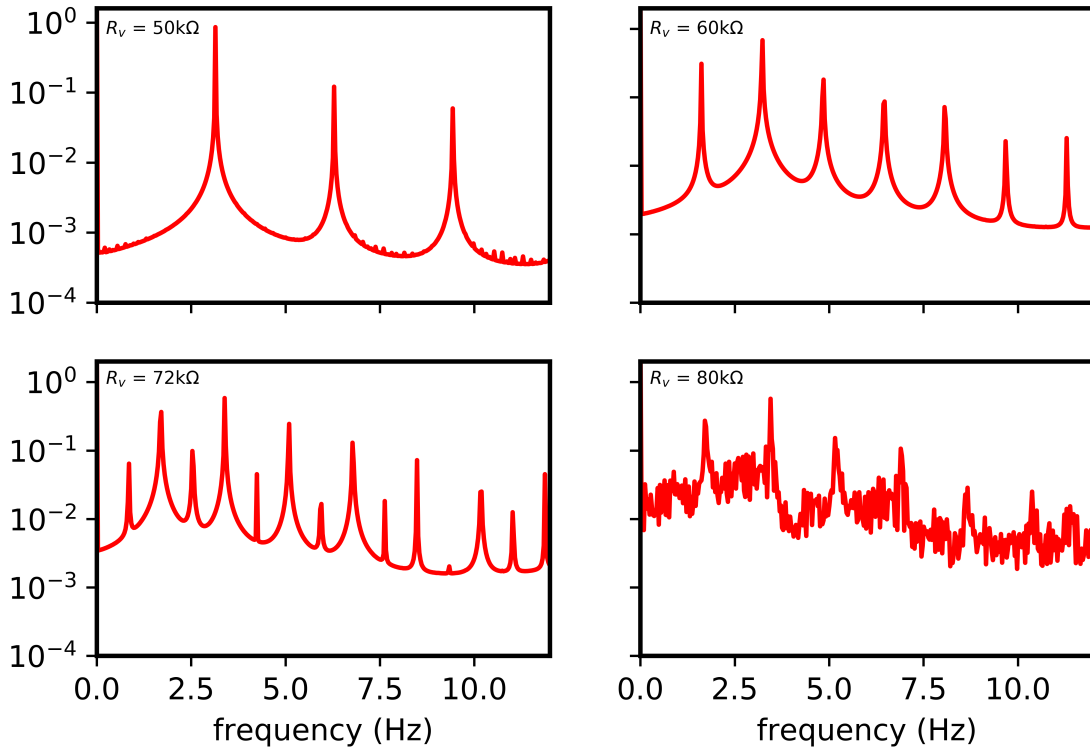


Figure 13: Experimental power spectra for four different values of R_v , 50 $k\Omega$, 60 $k\Omega$, 72 $k\Omega$, and 80 $k\Omega$. We see period doubling as the amount of peaks double as R_v increases. The 80 $k\Omega$ case is chaotic where its energy is spread out across the circuit so it is harder to see any definitive peaks.

One characteristic that is common throughout each power spectra is there is a definitive peak at approximately 3.1 Hz. The harmonic peaks in the 50 $k\Omega$ power spectra suggest that the oscillations are imperfectly sinusoidal. If we look at the spectra for 60 $k\Omega$ we see that there is an additional peak at half of the dominant frequency demonstrating that period doubling is also frequency halving, further emphasized in the 72 $k\Omega$ spectra.

4.3. Return Maps

Another way to visualize chaos by constructing a return map which is made by plotting the peak vs. the previous peak of the time series. The benefit of using this analysis is that it is a discrete, one-dimensional map of chaos. Our return map is for $R_v = 80 k\Omega$ Figure 15. The return maps match up fairly well to the theoretical curves, however, we see that there are some data points away from the experimental curve. These outlier points are essentially false peaks that are caused by noise in the time series.

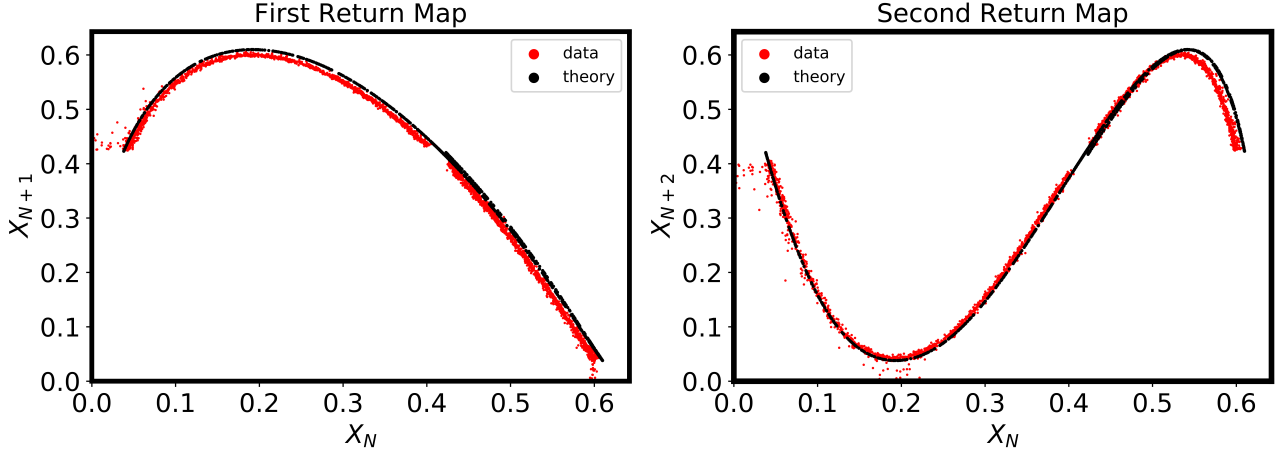


Figure 14: Return maps for the $80 \text{ k}\Omega$ chaotic state.

4.4. Bifurcation Diagram

To see every output of the system we can construct a bifurcation diagram, which is a graph showing all possible values for the varying initial conditions. The stable regions of our system are the white sections, where we saw forking and a fixed number of values. For example, stable regions appear from $50 \text{ k}\Omega$ to $72 \text{ k}\Omega$. However, the chaotic regions of the circuit are the values of R_v that form the bands that are filled with points.

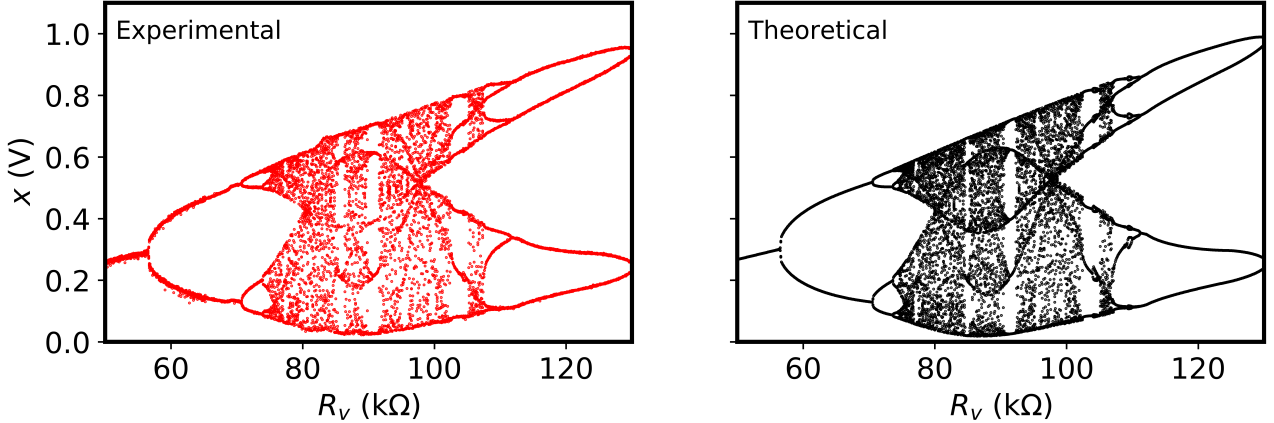


Figure 15: Bifurcation diagram

4.5. Lyapunov Exponent

Lyapunov exponents measures the rate of separation of close trajectories. A positive value implies chaos, while a negative value implies a fixed point or periodic cycle. Three Lyapunov exponents can be found per state of the system however we only looked at the largest since it is the best indicator of predictability. The theoretical value for the chaotic state of $80 \text{ k}\Omega$ was $1.96/\text{s}$. With the current version of the circuit, there is still too much noise to accurately obtain a experimental Lyapunov exponent. Current methods we are looking at to reduce noise include changing the types of diodes to low-noise models, and test different power supplies.

5. Conclusion

All experimental analyses corresponded closely with the theoretical expectations. A clear area of focus for future research, is to reduce the noise of the circuit. By reducing noise it allows for an increase in accuracy between the experimental data and the ODEs, and allows for the completion of more analyses. A reduction in noise would make it easier to solve for the experimental Lyapunov exponent and to visualize fractals in the

bifurcation diagram and return maps. With the current iteration of the chaotic circuit, it serves as an excellent tool to help students study chaotic systems and to act as a departing point into the vast field of chaos theory. The skills and techniques learned from experiments involving the chaotic circuit can be applied to many areas across physics such as weather, astronomy, and oceanography.

References

- [1] A. Aharony, "Fractals in Physics," *Europhysics news* **17**, 41 (1986).
- [2] A. Motter, D. Campbell, "Chaos at fifty," *Phys. Today* **66**, 27 (2013).
- [3] E. Lorenz, "Deterministic Nonperiodic Flow," *Journal of the Atmospheric Sciences*, **20**, 130, (1963).
- [4] H. Kantz, T. Schreiber, *Nonlinear Time Series Analysis*, 2nd edition (Cambridge University Press, New York, 2004).
- [5] J. Gleick, *Chaos: Making a New Science*, (Penguin Group, 1988).
- [6] J.C. Sprott, "Precision measurements of a simple chaotic circuit," *Am. J. Phys.* **72**, 503 (2004).
- [7] J.C. Sprott, *Chaos and Time-Series Analysis*, (Oxford University Press, Oxford, United Kingdom, 2003).
- [8] P. Horowitz, W. Hill, *The Art of Electronics*, (Cambridge University Press, 1980).
- [9] S. Strogatz, *Nonlinear Dynamics and Chaos*, (Perseus Books Publishing, 1994).